THE ASTROPHYSICAL JOURNAL, 397:117–125, 1992 September 20

THE He I λ2.06 MICRONS/Brγ RATIO IN STARBURST GALAXIES—AN OBJECTIVE CONSTRAINT ON THE UPPER MASS LIMIT TO THE INITIAL MASS FUNCTION

RENÉ DOYON[1]
Astrophysics Group, Blackett Laboratory, Imperial College, London, SW7 2BZ, England
P. J. PUXLEY[2]
Institute for Astronomy, 2680 Woodlawn Drive, Honolulu, HI 96822
AND
R. D. JOSEPH
NASA Infrared Telescope Facility, Institute for Astronomy, 2680 Woodlawn Drive, Honolulu, HI 96822
Received 1991 April 18; accepted 1992 March 24

ABSTRACT

The use of the He I λ2.06 μm/Brγ ratio as a constraint on the massive stellar population in star-forming galaxies is developed. A theoretical relationship between the He I λ2.06 μm/Brγ ratio and the effective temperature of the exciting star in H II regions is derived. The effects of collisional excitation and dust within the nebula on the ratio are also considered. It is shown that the He I λ2.06 μm/Brγ ratio is a steep function of the effective temperature, a property which can be used to determine the upper mass limit of the initial mass function (IMF) in galaxies. This technique is reliable for upper mass limits less than $\sim 40\ M_\odot$. New near-infrared spectra of starburst galaxies are presented. The He I λ2.06 μm/Brγ ratios observed imply a range of upper mass limits from 27 to $\gtrsim 40\ M_\odot$. There is also evidence that the upper mass limit is spatially dependent within a given galaxy. These results suggest that the upper mass limit is not a uniquely defined parameter of the IMF and probably varies with local physical conditions.

Subject headings: galaxies: ISM — galaxies: luminosity function, mass function — galaxies: starburst — infrared: galaxies

1. INTRODUCTION

The initial mass function (IMF), that is, the number of stars formed per unit mass interval, is a fundamental ingredient of star formation theories. The knowledge of the shape of this function is a prerequisite to understanding galaxy evolution and interpreting the properties of galaxies experiencing vigorous star formation activity (starburst). The IMF is usually described by a power law of the mass ($\psi \propto m^{-\alpha}$) and can be inferred from the "present-day mass function" derived from star counts in star clusters (Mateo 1988) or in the solar neighborhood (e.g., Miller-Scalo 1979). For instance the Salpeter IMF (1955) is described by an index $\alpha = 2.35$, whereas Scalo (1986) uses a three-segment power law, the upper end of the IMF ($0.7\ M_\odot \leq m \leq 100\ M_\odot$) having an index $\alpha \approx 2.85$.

Whether the solar neighborhood IMF is universal and whether it varies with physical conditions (metallicity, star formation rate) are still open questions (see Scalo 1986, 1987 and Zinnecker 1987 for reviews). However, there is growing observational evidence that the IMF is "unusual" in starburst galaxies. This is exemplified by several studies. From ultraviolet (UV) observations of several starbursts, Sekiguchi & Anderson (1987) concluded that the IMF slope is significantly flatter than the solar neighborhood value, that is, the IMF is selectively enriched in OB stars. A similar result was also obtained in the optical by Kennicutt et al. (1987). Gehrz, Sramek, & Weedman (1983) concluded that the observational properties of the starburst system NGC 3690–IC 694 are best explained if the IMF is deficient in high-mass stars ($>25\ M_\odot$). At the other end of the IMF, several infrared studies (Rieke et al. 1980; Wright et al. 1988; Puxley et al. 1989) suggest that starbursts are deficient in low-mass stars, or equivalently that the lower mass limit, m_l, is unusually high. Scalo (1989) has reviewed the evidence for a truncated IMF in starburst galaxies and pointed out that the conclusion above is valid only if the upper mass limit, m_u, is not significantly higher than 80–100 $M_\odot$. Unfortunately, the upper mass limit is probably the least constrained parameter of the IMF, and only a few studies (Puxley et al. 1989; Olofsson 1989) have provided quantitative constraints on this parameter.

In this paper we present a new and objective method for constraining the upper mass limit of the IMF which makes use of near-infrared (IR) recombination lines of helium and hydrogen, more specifically, the He I λ2.06 μm and Brγ (2.17 μm) transitions. New observations and data from the literature are combined to show that the upper mass limit inferred for some galaxies is relatively low. The new data are presented in § 2. The dependence of the He I λ2.06 μm/Brγ ratio on spectral type is derived in § 3, and its implications on the upper mass limit of the IMF are discussed in § 4. The main conclusions of this study are summarized in § 5.

2. OBSERVATIONS AND RESULTS

Near-infrared spectra of star-forming galaxies were obtained on the 3.8 m United Kingdom Infrared Telescope (UKIRT). These data were obtained as part of an observing program to determine the IR spectroscopic properties of starburst galaxies. A more detailed presentation of the data will be given elsewhere (Doyon et al. 1992). The sample includes interacting, merging, and dwarf galaxies for which IR "activity" has been identified in previous studies, either from photometric or spectroscopic observations. Although these galaxies differ in mor-

[1] Present address: Département de physique, Université de Montréal, C.P. 6128, Succ. A., Montréal (QC), Canada H3C 3J7.
[2] Present address: Royal Observatory, Blackford Hill, Edinburgh, EH9 3HJ, Scotland.

phology and bolometric luminosity, they all exhibit strong Brγ emission in their K-window spectra. None of the galaxies show clear evidence for nonthermal activity typical of active galactic nuclei (AGNs). NGC 1614 and He 2-10 are the only two potential "hard-spectrum" objects in our sample. The broad He II λ4686 emission-line feature detected in these sources is suggestive of the presence of numerous Wolf-Rayet (WR) stars (Conti 1991).

Except for He 2-10, all galaxies were observed during two observing runs in 1990 February and May. The K-window spectra were obtained with CGS2, the common-user seven-element cooled grating spectrometer of UKIRT. A circular aperture of 5″ was used for all sources and centered on the galaxy, either by peaking up the signal from the seven detectors or by setting the aperture on the optical nucleus as seen in the TV camera of the guiding system. The telescope was chopped between the target and the sky every grating position at a frequency of $\sim$1 Hz with chop throws of 30″. The spectra were sampled every half a resolution element. The wavelength scale of the instrument was calibrated at the beginning of each night by taking a spectrum of an argon lamp and/or a planetary nebula.

In order to take out periodic ripples due to the imperfect differential response of the detectors, the spectra were smoothed with a 1-2-1 triangular filter. Although this degraded the original resolution by about a factor of 2, this procedure ensured that no systematics were present in the spectra. A resolving power ($\lambda/\Delta\lambda$) of 300 $\pm$ 30 was derived from the width of Brγ as observed in absorption and emission in early-type stars and galaxies, respectively.

Atmospheric absorption features were corrected by dividing the galaxy spectra with the spectrum of a standard star obtained at a similar air mass ($\Delta AM < 0.1$–0.2). Early-type stars were used for this purpose since they have a featureless continuum except for the Brγ absorption at 2.1661 μm which was removed by interpolating across the raw spectrum. The spectra were then multiplied by a blackbody spectrum with effective temperature and absolute flux specified by the spectral type and the K magnitude of the standard star.

The observations of He 2-10 were made in 1989 November on UKIRT using CGS2 with a 5″ aperture centered on the optical nucleus. The spectrum consisted of six co-adds, each of four samples of 1 s at each grating position. The scans were made in stare mode, running through each grating position on the source and then offsetting 57″ east or west to repeat the scan. The data were sampled at one third of a resolution element with a resolving power of $\sim$700. The spectrum of the galaxy was ratioed with that of BS3425 (K5III), both obtained at a similar air mass. Because of its higher quality, the spectrum of He 2-10 was not corrected by the smoothing technique described above.

The spectra are shown on a relative scale in Figure 1, shifted to the galaxies' rest frames using the redshifts derived from the position of Brγ in the spectra. Most galaxies show strong unresolved He I λ2.06 μm and Brγ lies in their spectra. Other emission lines are also detected, the most conspicuous being those of molecular hydrogen [e.g., 1 – 0 $S(1)$ at 2.122 μm]. The origin and excitation mechanism of the H_2 emission will be discussed in a subsequent paper (Doyon et al. 1992).

Brγ fluxes, measured by fitting a Gaussian profile to the line, and He I λ2.06 μm/Brγ ratios are given in Table 1. The latter were not corrected for the differential extinction between 2.06 and 2.16 μm since this is very small. For example, a visual extinction as high as 20 mag implies a change in the line ratio of only 20%. Note that the error quoted for these ratios includes the uncertainty in placing the continuum level. Data for other galaxies, taken from the literature, are also included. The He I λ2.06 μm/Brγ ratios are typically between 0.3 and 0.6.

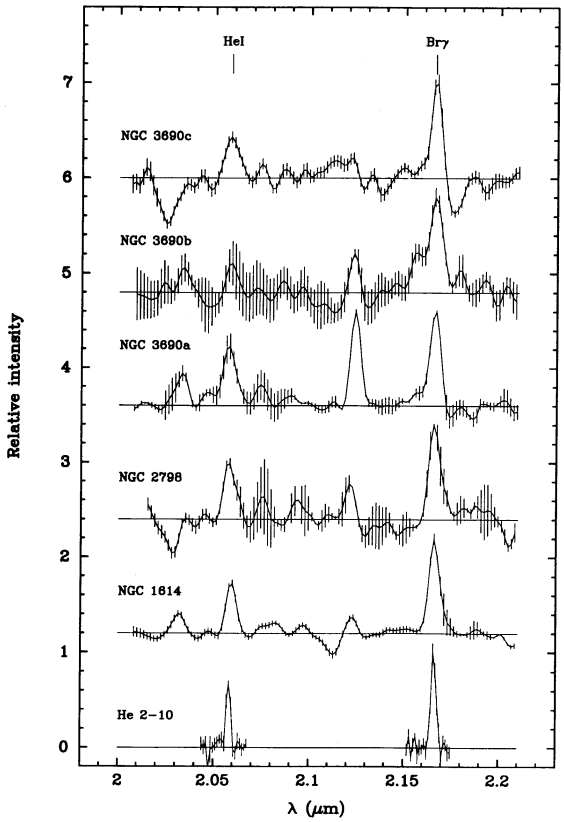

FIG. 1.—K-window spectra of star-forming galaxies. Spectra are shown in their restframe on a relative intensity scale, separated from each other by a unit of 1.2. Spectra have been continuum-subtracted and normalized such that Brγ has a peak intensity of unity.

Since the ionization potential of helium is twice that of hydrogen, the detection of the He I λ2.06 μm line shows without doubt that an intense and hot UV field is present in these nuclei. Without any evidence for AGN-type activity in these galaxies, one is forced to conclude that the UV photons are produced by a population of young OB stars. This conclusion is also valid for "WR galaxies." Even though WR stars could, in principle, contribute significantly to the total ionization balance, in practice their contribution is very modest compared with O stars because of the small WR/O star ratio (near 0.1) expected for a normal IMF (Maeder 1990). We will thus assume in the following analysis that the emission-line spectrum of the galaxies is due primarily to OB stellar photoionization.

Because the ionization rate has a strong dependence on stellar effective temperature ($T_{\rm eff}$), the He I λ2.06 μm/Brγ ratio, which is basically determined by the ratio of the production rate of UV photons with energy greater than 24.6 and 13.6 eV (the ionization potentials of helium and hydrogen, respectively), will also have a strong dependence on spectral type. In principle, this property can be used to constrain the relative number of massive stars in the stellar population of a starburst, and this in turn can be translated into a constraint

TABLE 1

OBSERVATIONAL PROPERTIES OF THE GALAXIES

Galaxy Name (1)	D[a] (Mpc) (2)	$F_{Br\gamma}$[b] (3)	Ap (4)	He I/Brγ (5)	m_u ($M_\odot$) (6)	Reference[c] (7)
He 2-10	15	6.5 ± 0.7	5″	0.64 ± 0.09	$51^{>49}_{-18}$	This work
NGC 253	3	65 ± 7	7.8	0.38 ± 0.08	29^{+5}_{-1}	1
M82	3	20 ± 0.4	3.8	0.34 ± 0.02	28^{+2}_{-1}	2
NGC 1614	63	6.0 ± 0.2	5	0.55 ± 0.05	36^{+27}_{-5}	This work
NGC 2798	23	2.2 ± 0.2	5	0.60 ± 0.08	42^{+58}_{-10}	This work
NGC 3256 A[d]	37	5.4 ± 0.1	3.5	0.33 ± 0.04	28 ± 2	3
NGC 3256 B[d]	37	1.6 ± 0.2	3.5	0.71 ± 0.15	>34	3
NGC 3690 A	40	3.7 ± 0.1	5	0.65 ± 0.08	$54^{>46}_{-20}$	This work
NGC 3690 B	40	1.9 ± 0.1	5	0.28 ± 0.05	27 ± 2	This work
NGC 3690 C	40	3.7 ± 0.1	5	0.48 ± 0.05	32^{+8}_{-3}	This work

[a] Assuming $H_0 = 75$ km s^{-1} Mpc^{-1}.
[b] Observed Brγ flux in units of 10^{-17} W m^{-2}, uncorrected for extinction.
[c] References: (1) Rieke et al. 1988; (2) Lester et al. 1990; (3) Doyon 1991; Doyon et al. 1992.
[d] NGC 3256 A: nucleus NGC 3256 B: average of two positions 5″ east and south of the nucleus.

on the upper mass limit of the IMF. In order to quantify this constraint, we examine in the following sections the theoretical relationship between the He I λ2.06 μm/Brγ ratio and $T_{\rm eff}$, and also investigate the possible physical processes that could affect this ratio.

3. THE He I λ2.06 μm/Brγ RATIO IN H II REGIONS

3.1. *The* He I λ2.06 μm/Brγ *Ratio vs.* $T_{\rm eff}$

The ionization structure of an H II region surrounding an O star consists primarily of an inner He^+ zone with a volume V_{He^+} smaller than or equal to V_{H^+}, the volume of the H^+ zone. Thus the He I λ2.06 μm/Brγ ratio will depend strongly on the relative size of the two ionized zones which in turn depends on the effective temperature of the exciting star. The He I λ2.06 μm/Brγ ratio can be determined analytically by making the following assumptions and approximations: (1) the ionized gas is optically thick to the Lyman lines and continuum, the usual case B approximation, and (2) hydrogen has a negligible contribution to the opacity in the He^+ zone that is, all photons produced by ground-state recombinations of He I are consumed by He I reionization. This is the equivalent case B approximation for helium. The luminosity emitted in each line is then given by

$$L_{Br\gamma} = h\nu_{Br\gamma} N_{H^+} \alpha^{\rm eff}_{Br\gamma}[N_e^{He^+} V_{He^+} + N_e^{H^+}(V_{H^+} - V_{He^+})] \quad (1a)$$

$$L_{He\,I\,\lambda2.06} = h\nu_{He\,I\,\lambda2.06} N_{He^+} N_e^{He^+} \alpha^{\rm eff}_{He\,I\,\lambda2.06} V_{He^+}, \quad (1b)$$

where $N_e^{H^+}$ and $N_e^{He^+}$ are the electron densities in the H^+ and He^+ zones, respectively. N_{H^+} and N_{He^+} are the number densities of H^+ and He^+ $\alpha^{\rm eff}_{He\,I\,\lambda2.06}$ and $\alpha^{\rm eff}_{Br\gamma}$ are the effective recombination coefficients of the He I λ2.06 μm and Brγ transitions, respectively.

Since species other than hydrogen and helium have a negligible contribution to the electron density, then, to a very good approximation, $N_e^{He^+} = N_{He^+} + N_{H^+}$ and $N_e^{H^+} = N_{H^+}$. The He I λ2.06 μm/Brγ ratio is then given by

$$\frac{I_{He\,I\,\lambda2.06}}{I_{Br\gamma}} = \frac{\lambda_{Br\gamma}}{\lambda_{He\,I\,\lambda2.06}} \frac{\alpha^{\rm eff}_{He\,I\,\lambda2.06}}{\alpha^{\rm eff}_{Br\gamma}} \frac{(1+Y)YR}{1+YR}, \quad (2)$$

where $Y \equiv N_{He^+}/N_{H^+}$, the helium abundance by number and $R \equiv V_{He^+}/V_{H^+}$. The parameter R is a function of $N^{He^+}_{Lyc}(T_{\rm eff})$ and $N^{H^+}_{Lyc}(T_{\rm eff})$, the production rates of ionizing photons with energy greater than 24.6 and 13.6 eV, respectively, for a star with effective temperature $T_{\rm eff}$. Following a similar argument used for deriving equation (1), it is easy to show that

$$\frac{N^{He^+}_{Lyc}(T_{\rm eff})}{N^{H^+}_{Lyc}(T_{\rm eff})} = \frac{\alpha_B(He^+)}{\alpha_B(H^+)} \frac{(1+Y)YR}{1+YR}, \quad (3)$$

where $\alpha_B(H^+)$ and $\alpha_B(He^+)$ are the total recombination coefficients for hydrogen and helium in the case B approximation. Above a certain critical effective temperature $T^c_{\rm eff}$, the He I λ2.06 μm/Brγ ratio becomes independent of the effective temperature and saturates to a value obtained from equation (2) by setting $R = 1$. Below $T^c_{\rm eff}$ the ratio is simply given by combining equations (3) and (2). We note that, in this case, the ratio is independent of the helium abundance and specified directly from the ionization rate ratio $N^{He^+}_{Lyc}/N^{H^+}_{Lyc}$.

The effective recombination coefficient $\alpha^{\rm eff}_{He\,I\,2.06}$ is the only quantity which is not directly available from the literature. However, this coefficient can be indirectly estimated from other line ratios using the following expressions:

$$\alpha^{\rm eff}_{He\,I\,2.06} = \alpha^{\rm eff}_{\lambda4471} \frac{I_{He\,I\,\lambda2.06}}{I_{\lambda4471}} \frac{\lambda_{He\,\lambda2.06}}{\lambda_{4471}} \quad (4a)$$

$$\alpha^{\rm eff}_{He\,I\,\lambda2.06} = \alpha^{\rm eff}_{Br\gamma} \frac{N_{H^+}}{N_{He^+}} \frac{I_{He\,I\,\lambda2.06}}{I_{\lambda4471}} \frac{I_{H\beta}}{I_{Br\gamma}} \frac{I_{\lambda4471}}{I_{H\beta}} \frac{\lambda_{He\,I\,206}}{\lambda_{Br\gamma}}, \quad (4b)$$

where $I_{\lambda4471}$ is the intensity of a triplet transition of helium at 4471 Å. Treffers et al. (1976) have estimated that the ratio $I_{He\,I\,\lambda2.06}/I_{\lambda4471}$ should be equal to 0.65 if the nebula is optically thick in the 2^1P–1^1S resonant transition of helium at 584 Å (see Fig. 4). Taking $\alpha^{\rm eff}_{\lambda4471}$ from Brocklehurst (1972)[3] for an electron temperature and density of 10^4 K and 10^4 cm^{-3}, respectively, equation (4a) yields $\alpha^{\rm eff}_{He\,I\,2.06} = 4.03 \times 10^{-14}$ cm^3 s^{-1}. For the same conditions, the $I_{H\beta}/I_{Br\gamma}$ ratio is predicted to be 36.4 under case B (Hummer & Storey 1987). Following

[3] Brocklehurst gives the coefficient for case A only, and we assume the same coefficient for case B. This should be a reasonable approximation since λ4471 is weakly affected by optical depth effects.

Wynn-Williams et al. (1978), the I_{4471}/I_{H_β} ratio can be empirically determined from observations of H II regions. This ratio is typically 0.04 in optically visible H II regions (Peimbert & Torres-Peimbert 1971, as quoted by Wynn-Williams et al.). Taking $\alpha^{\rm eff}_{{\rm Br}\gamma}$ as derived from Hummer & Storey (1987) and assuming an helium abundance of 10%, typical for Galactic H II regions, equation (4b) gives $\alpha^{\rm eff}_{{\rm He\,I}\,2.06} = 3.36 \times 10^{-14}$ cm^3 s^{-1} which is slightly lower than the value predicted from equation (4a). We adopt the average of the two values and assign an arbitrary uncertainty of $\sim$10% on $\alpha^{\rm eff}_{{\rm He\,I}\,2.06}$ bearing in mind that this uncertainty could well be underestimated.

This coefficient must be corrected for the fact that not all resonant 584 Å photons are recycled by helium. Although these photons are unlikely to escape the nebula, they can ionize hydrogen, and this process will compete with the scattering due to helium. As shown by Thompson & Tokunaga (1980), the absorption cross section of helium is $\sim 2.5 \times 10^4$ higher than the photoionization cross section of hydrogen at 584 Å. Taking into account the fact that helium is less abundant than hydrogen, 584 Å photons have a probability of 0.0005 of being destroyed by hydrogen atoms. Since the 2^1P state has a probability of 0.001 of decaying to the 2^1S, only $\frac{2}{3}$ of the helium atoms in the 2^1P state will give rise to a 2.06 μm photon. Thus the effective recombination coefficient $\alpha^{\rm eff}_{{\rm He\,I}\,\lambda 2.06}$ must be multiplied by a factor $\frac{2}{3}$. It should be noted that the exact value of the "$\frac{2}{3}$ factor" critically depends on the relative number of neutral hydrogen and helium atoms in the He^+ zone. If hydrogen is relatively more ionized than helium, then most 584 Å photons will be absorbed by ground state neutral helium atoms, in which case the "$\frac{2}{3}$ factor" would be better replaced by unity. Without any evidence that this is indeed the case, we adopt a value of $\frac{2}{3}$ for the correction factor of $\alpha^{\rm eff}_{{\rm He\,I}\,\lambda 2.06}$. We shall discuss the implications of this uncertainty on the main results of the paper later in § 4.

Finally, using $\alpha_B(H^+)$ from Hummer & Storey (1987) and $\alpha_B(He^+)$ from Osterbrock (1989) for the same temperature and density as above, equations (2) and (3) yield

$$\frac{I_{\rm HeI2.06}}{I_{{\rm Br}\gamma}} = 7.0Y \quad \text{if} \quad V_{He^+} = V_{H^+}\,,$$
$$\frac{I_{\rm HeI2.06}}{I_{{\rm Br}\gamma}} = 6.6\,\frac{N^{He^+}_{\rm Lyc}(T_{\rm eff})}{N^{H^+}_{\rm Lyc}(T_{\rm eff})} \quad \text{if} \quad V_{He^+} < V_{H^+}\,. \tag{5}$$

Puxley (1988; see also Puxley, Hawarden, & Mountain 1990) have integrated Kurucz (1979) atmosphere models, using the compilation of stellar properties of Landolt-Börnstein (1982), to calculate the ionization rate $N^{H^+}_{\rm Lyc}(T_{\rm eff})$. For consistency we calculated the ionization rates $N^{He^+}_{\rm Lyc}(T_{\rm eff})$ in the same way as prescribed by Puxley (1988). These numbers are compiled in Table 2 for stars with effective temperatures ranging from 8000 to 50,000 K.

The dependence of the He I λ2.06 μm/Brγ line ratio on effective temperature is shown in Figure 2. We adopted a Galactic helium abundance of 0.112 for consistency with that used by Kurucz (1979). For a Galactic abundance, the He^+ and the H^+ zones are coincident near a temperature of $\sim$38,000 K, corresponding to an O7V star (Landolt-Börnstein 1982). These simple calculations show that *the* He I λ2.06 μm/Brγ *line ratio is very sensitive to spectral type.*

The validity of the analytical expressions derived above may be tested by comparison with the detailed calculations of Rubin (1985) who determined the size of both the He^+ and H^+ zones for different effective temperatures ranging from 31,000 to 45,000 K. The dependence of the ratio $R \equiv V_{He^+}/V_{H^+}$ as a function of effective temperature, as inferred from Rubin's calculations, is shown in Figure 3 (dashed lines and points). The solid curve was calculated using the "dust-free" ionization rates given in Table 1 and the following analytical expression

TABLE 2

IONIZATION RATES FOR DUST-FREE AND DUSTY H II REGIONS

Mass ($M_\odot$)	$T_{\rm eff}$ (K)	Sp.	DUST-FREE H II REGIONS log $N^{H^+}_{\rm Lyc}$ (s^{-1})	DUST-FREE H II REGIONS log $N^{He^+}_{\rm Lyc}$ (s^{-1})	"DUSTY" H II REGIONS[a] log $N'^{H^+}_{\rm Lyc}$ (s^{-1})	"DUSTY" H II REGIONS[a] log $N'^{H^+}_{\rm Lyc}$ (s^{-1})	$\tau_{\rm eff}$[b]
1.9	8000	A6V	34.01	23.41	34.01	23.41	0.00
2.2	8500	A4V	35.08	25.01	35.08	25.01	0.00
2.5	9000	A2V	36.43	26.47	36.43	26.47	0.00
2.9	9500	A0V	37.46	27.73	37.46	27.73	0.00
3.1	10000	B9.5V	38.22	28.94	38.22	28.94	0.00
3.5	11000	B9V	39.24	31.03	39.24	31.03	0.00
3.9	12000	B8V	40.05	32.56	40.05	32.56	0.00
4.5	13000	B7V	40.79	34.12	40.79	34.12	0.00
5.1	14000	B6V	41.43	35.27	41.43	35.27	0.00
5.7	15000	B5V	42.02	36.44	42.02	36.44	0.00
6.2	16000	B4.5V	42.57	37.44	42.57	37.44	0.01
6.7	17000	B4V	43.11	38.30	43.10	38.30	0.01
7.2	18000	B3.5V	43.58	39.04	43.57	39.04	0.01
8.5	20000	B2.5V	44.35	40.37	44.34	40.37	0.02
10.3	22500	B2V	45.17	41.63	45.15	41.62	0.04
12.6	25000	B1V	45.92	42.88	45.89	42.86	0.08
17.5	30000	B0V	47.26	45.22	47.18	45.18	0.20
21.9	35000	O8V	48.34	46.93	48.17	46.85	0.41
34.3	40000	O6.5V	49.03	48.29	48.78	48.18	0.56
63.8	45000	O5V	49.46	48.90	49.17	48.75	0.67
101.2	50000	O3.5V	49.84	49.36	49.50	49.19	0.78

[a] Calculated with $n_{\rm H} = 10\,{\rm cm}^{-3}$, typical of optically visible H II regions.
[b] Defined such that $N'^{H^+}_{\rm Lyc} = N^{H^+}_{\rm Lyc} \exp(-\tau_{\rm eff})$.

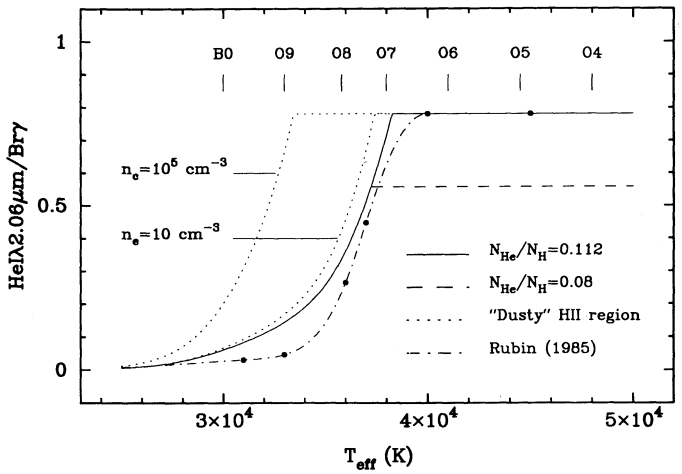

FIG. 2.—He I λ2.06 μm/Brγ ratio vs. effective temperature, calculated for a Galactic (*solid line*) and primordial (*dashed line*) helium abundance. The dotted lines show the effect of internal dust on the line ratio for two electron densities and a Galactic helium abundance. The lower density is typical of optically visible H II regions.

derived directly from equation (3):

$$R^{-1} = \frac{\alpha_B(\mathrm{He}^+)}{\alpha_B(\mathrm{H}^+)} \frac{N_{\mathrm{Lyc}}^{\mathrm{H}^+}(T_{\mathrm{eff}})}{N_{\mathrm{Lyc}}^{\mathrm{He}^+}(T_{\mathrm{eff}})} (1 + Y)Y - Y \, . \qquad (6)$$

Figure 3 shows that both models are reasonably in good agreement. They both show a steep dependence of R with effective temperature and predict a similar critical temperature at which $R = 1$.

Because of its simplicity, we shall retain the analytical model for investigating the effect of internal dust on the He I λ2.06 μm/Brγ ratio of H II regions (see § 3.3), but we shall use Rubin's calculations for predicting the integrated line emission from a ensemble of stars.

3.2. *Collisional Excitation*

Beyond a critical density of (3–5) × 10^3 cm^{-3}, the 2^3S metastable level (see Fig. 4) is preferentially collisionally depopulated to the 2^1S and 2^1P levels rather than by the forbidden single-photon decay at 19.8 eV (626 Å). This, of course, enhances the strength of a 2.06 μm transition. Osterbrock (1989) estimates that 17% of all the captures to 2^3S lead to 2^1P. Since three quarters of all helium recombinations end up as 2^3S and approximately $\frac{2}{3}$ of the singlet captures (one quarter of all recombinations) lead to 2^1P, compared with the low-density regime, collisional excitation will overpopulate the 2^1P level by a factor 1.8. Thus, if the density is high enough, the theoretical He I λ2.06 μm/Brγ ratio derived earlier will be enhanced by this factor. However, for typical bright H II regions in which $n_e \lesssim 10^2$ cm^{-3}, this effect should be negligible.

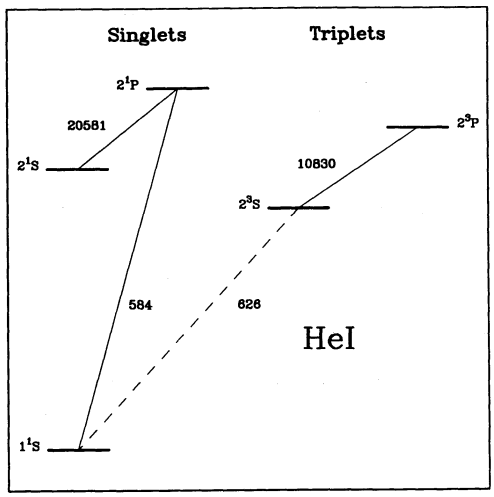

FIG. 4.—Partial energy-level diagram of He I. Selected transitions are indicated by their wavelength in Å. Vertical axis is not to scale.

The fact that most galaxies in Table 1 have He I λ2.06 μm/Brγ ratios lower than the saturated value of 0.8, calculated for the low-density regime, suggests that collisional excitation is probably negligible is these galaxies. This, in turn, places an upper limit for the electron density of the photoionized gas to (3–5) × 10^3 cm^{-3}, much lower than the typical density of ~10$^{4-5}$ cm^{-3} inferred in ultracompact H II regions (Wood & Churchwell 1989). Although very speculative, this suggests that the H II regions responsible for the observed near-IR recombination lines in starburst galaxies are relatively evolved.

3.3. *Effect of Dust within the* H II *Regions*

Dust is certainly present in H II regions. It is clearly evident from their optical photographs but also from the infrared excess inferred in these objects (Wynn-Williams et al. 1978; Chini, Krügel, & Wargau 1987; Wood & Churchwell 1989). Dust particles compete with hydrogen in absorbing ionizing photons. The magnitude of this effect can be judged by comparing the ionization rates derived from the bolometric luminosity (from the far-infrared *IRAS* flux) and the free-free radio flux. In their study of compact H II regions, Wood & Churchwell (1989) showed that between 50% and 90% of the ionizing photons are absorbed by dust. This result is consistent with predictions from models of "dusty" H II regions (e.g., Mathis 1986).

Because the dust absorption cross section is not constant beyond 13.6 eV (Draine & Lee 1984), the relative ionization rates, $N_{\mathrm{Lyc}}^{\mathrm{H}^+}$ and $N_{\mathrm{Lyc}}^{\mathrm{He}^+}$, will be affected by the presence of dust, and therefore the He I λ2.06 μm/Brγ line will also change (see eq. [5]). In this section we quantify the magnitude of this effect

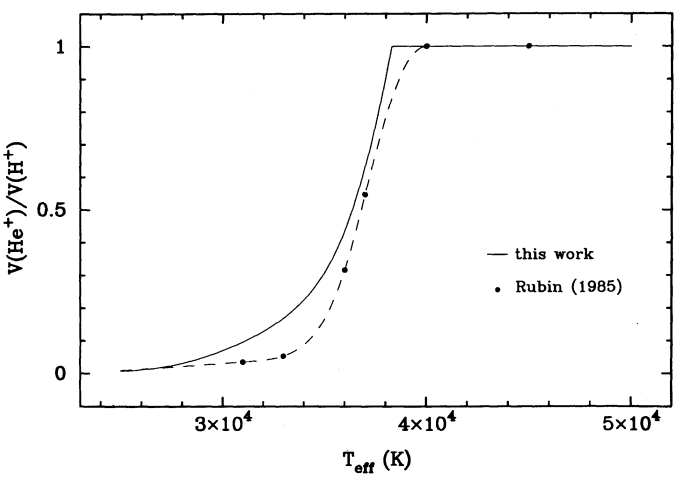

FIG. 3.—Volume ratio of the He^+ and H^+ zones as a function of effective temperature in an H II region. The solid curve is the prediction from the analytical model (eq. [6]) described in the text. The solid points were taken from the detailed ionization structure calculations of Rubin (1985). The dashed line represents the adopted interpolation.

using a simple description of a "dusty" H II region based on the analytical model described earlier. The following is also partly based on the model described by Mathis (1986).

In order to estimate how the ionization rates are affected by the presence of dust, the wavelength dependence of the dust absorption must be determined. The increment of optical depth at wavelength λ, corresponding to an increment in geometric path length dr, and due to grains with radii in the interval $[a, a + da]$, is given by

$$d\tau_\lambda = \sigma_d(\lambda, a) dn_d(a) dr \,, \quad (7)$$

where $\sigma_d(\lambda, a)$ is the dust absorption cross section, $dn_d(a)$ the number density of dust particles with radii in the interval $[a, a + da]$ as defined in equation (9) and r the distance from the source. Here $\sigma_d(\lambda, a)$ is related to the grain radius a via the following expression:

$$\sigma_d(\lambda, a) = \pi a^2 Q_{\rm abs}(a, \lambda) \,, \quad (8)$$

where $Q_{\rm abs}(a, \lambda)$ is the absorption efficiency. For $dn_d(a)$, we adopt the grain size distribution of Mathis, Rumpl, & Nordsieck (1977), which includes both silicate and graphite particles:

$$dn_d(a) = (A_{\rm sil} + A_{\rm grap}) n_{\rm H} a^{-3.5} da \quad a_{\rm min} < a < a_{\rm max} \,, \quad (9)$$

where $n_{\rm H}$ is the gas number density and $A_{\rm sil} = 10^{-25.11}$ cm$^{2.5}$/H, $A_{\rm grap} = 10^{-25.16}$ cm$^{2.5}$/H, $a_{\rm min} = 0.005$ μm, and $a_{\rm max} = 0.25$ μm (Draine & Lee 1984). For a grain density of 3.3 g cm^{-3}, this distribution corresponds to a dust-to-gas mass ratio of 10^{-2}. Equation (7) may be integrated over grain size and distance r, up to the Strömgren radius R_S, to obtain an expression for τ_λ. R_S is the Strömgren radius in the presence of dust which is related to the dust-free radius, R_0, in the following way: $R_S \approx R_0 \exp(-\tau_{\rm eff}/3)$. Here $\tau_{\rm eff}$ is the effective dust optical depth in the Lyman continuum defined such that $N'^{\rm H^+}_{\rm Lyc} = N^{\rm H^+}_{\rm Lyc} \exp(-\tau_{\rm eff})$ where $N'^{\rm H^+}_{\rm Lyc}$ is the ionization rate modified by the presence of dust. Using the usual definition for R_0, the integration of equation (7) yields

$$\exp(\tau_{\rm eff}/3)\tau_\lambda \approx 0.27[Q^{\rm sil}_{\rm abs}(\lambda) + 0.89 Q^{\rm grap}_{\rm abs}(\lambda)] \times \left(\frac{n_{\rm H}}{10\ {\rm cm^{-3}}}\right)^{1/3} \left(\frac{N^{\rm H^+}_{\rm Lyc}}{10^{49}\ {\rm s^{-1}}}\right)^{1/3} . \quad (10)$$

In evaluating the integral, we have assumed that all dust particles have the same absorption efficiency $Q_{\rm abs}$ given for a grain size of 0.01 μm. This is a reasonable approximation since $d\tau_\lambda/da$ varies as $\lambda^{-1.5}$, and thus only small particles of the order of 0.01 μm will contribute significantly to the integral.

Not surprisingly, τ_λ depends on the density and also on the luminosity of the exciting star via $N^{\rm H^+}_{\rm Lyc}$. Equation (10) has the uncomfortable and circular feature that in order to estimate τ_λ, one must also know $\tau_{\rm eff}$. This is due to our simplistic description of an H II region. To be rigorous, radiative transfer equations should be solved at every point in the nebula taking into account equation (7), but this is beyond the scope of this paper. We can circumvent this problem by the following approximation. For a given density and ionization rate, the average of the right-hand side of equation (10) may be calculated over wavelength; τ_λ on the left-hand side can then be replaced by $\tau_{\rm eff}$ which allows the equation to be solved for $\tau_{\rm eff}$.

We have calculated τ_λ for different effective temperatures and a density of 10 cm^{-3}, using the absorption efficiencies tabulated in Draine (1985) and the dust-free ionization rates given in Table 2. The dependence of the optical depth on wavelength is shown in Figure 5 for an O5 star. Since the optical depth peaks around 800 Å (15.5 eV), the presence of dust will have a stronger effect on $N^{\rm H^+}_{\rm Lyc}$ than on $N^{\rm He^+}_{\rm Lyc}$. Using the expression for τ_λ, we recalculated the ionization rates by integrating under Kurucz models, adding a factor $\exp(-\tau_\lambda)$ in the integral. The resulting ionization rates, $N'^{\rm H^+}_{\rm Lyc}$ and $N'^{\rm He^+}_{\rm Lyc}$, are tabulated in Table 2 along with the effective dust optical depth $\tau_{\rm eff}$. Typically between 30% and 50% of the ionizing photons beyond 13.6 eV are absorbed by dust, which is in fairly good agreement with previous models of dusty H II regions (e.g., Panagia 1974; Mathis 1986).

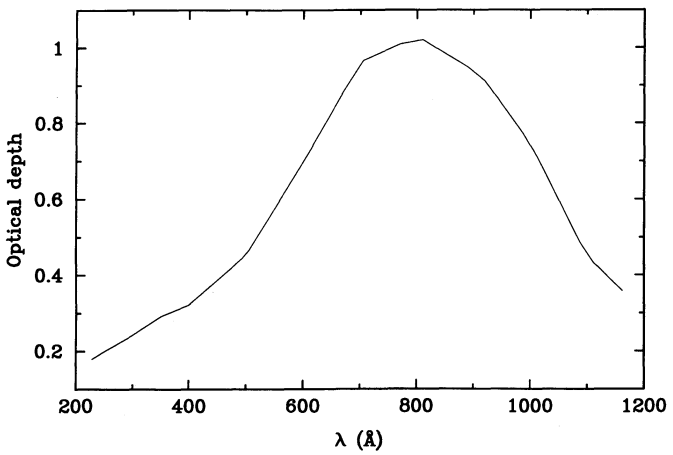

FIG. 5.—Wavelength dependence of the dust optical depth in the Lyman continuum, calculated for an H II region with $n_{\rm H} \approx n_e = 10$ cm^{-3} and an exciting star with effective temperature of 45,000 K (O5V).

These new ionization rates can now be used to calculate the He I λ2.06 μm/Brγ line ratio in dusty H II regions. The results are graphically displayed in Figure 2 (dotted lines). The main effect of the dust is to decrease the temperature at which the line ratio saturates, resulting in a steeper dependence between the He I λ2.06 μm/Brγ ratio and the effective temperature of the exciting star. This effect, however, is very small for typical H II regions with densities of $\lesssim 10$ cm^{-3} but cannot be neglected for high-density (10^{4-5} cm^{-3}) objects such as compact H II regions.

It is important to note that these results are valid only if we assume that the dust-to-gas ratio in H II regions is similar to that in the interstellar medium. Although graphite and silicate dust particles can survive the harsh environment of an H II region (Salpeter 1977), the inner region can still be swept clear of dust by radiation pressure (Osterbrock 1989). The dust content of an H II region could be reduced in this way. Dust depletion in H II regions has been noted in some sources (Tielens & de Jong 1979; Churchwell, Wolfire, & Wood 1990). A lower dust content would considerably reduce its effect on the He I λ2.06 μm/Brγ ratio. For instance, a bright H II region with $n_e = 10^2$ cm^{-3} and a normal dust-to-gas mass ratio would have the same He I λ2.06 μm/Brγ ratio as a compact H II region with $n_e = 10^5$ cm^{-3} and a dust-to-gas ratio reduced by a factor of 10, for the same exciting star.

Thus, although internal dust within H II regions can potentially affect the He I λ2.06 μm/Brγ ratio, the magnitude of this effect is difficult to judge without an accurate determination of the dust-to-gas ratio. However, the simple calculations above suggest that this effect should be very small in low-density and bright H II regions.

4. THE He I λ2.06 μm/Brγ RATIO IN GALAXIES

Having determined the dependence of the He I λ2.06 μm/Brγ ratio on effective temperature, we can now predict the integrated ratio associated with a young stellar population. If we assume that the star formation has been going on long enough at a steady state to establish an birth/death equilibrium population for the most massive stars, then the integrated He I λ2.06 μm/Brγ ratio, $I_{\rm He\,I}$, is simply given by

$$I_{\rm HeI} = \frac{\int_{m_l}^{m_u} L_{\rm Br\gamma}(m) I_{\rm HeI}(m) \psi(m) \tau(m) dm}{\int_{m_l}^{m_u} L_{\rm Br\gamma}(m) \psi(m) \tau(m) dm}, \qquad (11)$$

where $\psi(m)$ is the initial mass function with lower and upper mass limits m_l and m_u, respectively, and $\tau(m)$ is the lifetime of stars parameterized as $\tau(m) \propto m^{-0.59}$ for $13 < m < 100\ M_\odot$ (Puxley 1988). $L_{\rm Br\gamma}(m)$ is the Brγ luminosity of an H II region with an exciting star of mass m, calculated from the ionization rate assuming that one Brγ photon is emitted for every 70 Lyman continuum photons (Hummer & Storey 1987).

Because the ionization rate is a steep function of the mass (cf. Table 2), the integrated He I λ2.06 μm/Brγ ratio should be strongly dependent on the upper mass limit m_u but fairly insensitive to m_l (as long as it is lower than 10 $M_\odot$). Further, the integrated ratio is weakly sensitive to the slope of the IMF because the He I λ2.06 μm/Brγ varies rapidly over a small mass range. The dependence of $I_{\rm He\,I}$ on m_u is shown in Figure 6. This was calculated using equation (11) with a Salpeter IMF ($\psi \propto m^{-\alpha}$, $\alpha = 2.35$), $m_l = 0.1\ M_\odot$, and the He I λ2.06 μm/Brγ ratios derived from equation (2) with R taken from Rubin's calculations (see dashed line in Fig. 3).

The solid heavy lines in Figure 6 represent two different helium abundances, Galactic (upper curve) and primordial (lower curve). In order to take into account the uncertainty of the theoretical He I λ2.06 μm/Brγ ratio, equation (11) was also calculated using a Galactic helium abundance and an effective recombination coefficient, $\alpha^{\rm eff}_{\rm He\,I\,\lambda 2.06}$, 10% lower and higher than the average adopted in § 3.1. This case is represented by the two dashed lines in Figure 6. Despite these uncertainties, Figure 6 shows that the He I λ2.06 μm/Brγ ratio provides a reliable measure of the upper mass limit when the ratio is less than ~0.6, which is the case for half of the galaxies listed in Table 1. However, because of the saturation of the line ratio, this method is unreliable beyond $m_u \sim 40\ M_\odot$.

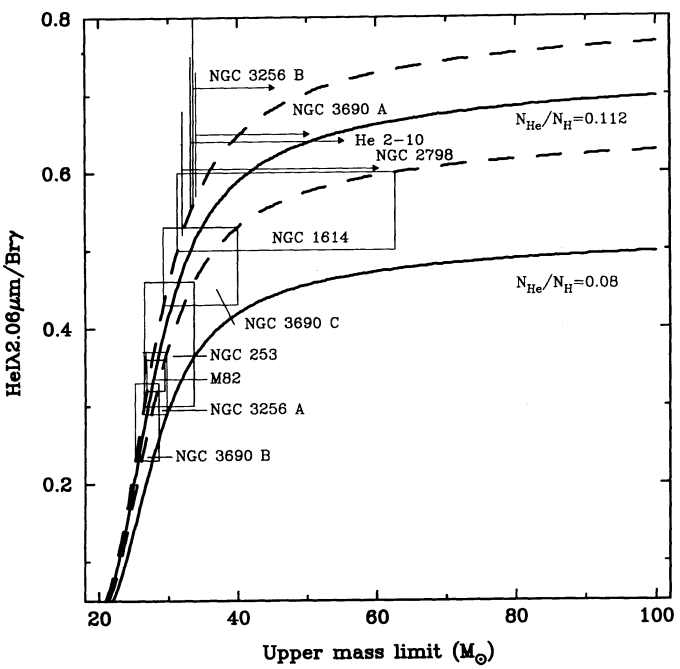

FIG. 6.—He I λ2.06 μm/Brγ ratio vs. upper mass limit m_u, calculated as described in the text for two helium abundances (*solid lines*). The dashed lines show the effect of varying the effective recombination coefficient, $\alpha^{\rm eff}_{\rm He\,I\,2.06}$, by ±10% (a Galactic helium abundance was assumed). Galaxies are represented either by a box with dimensions of the same size as the errors on both the line ratio and m_u or by an arrow showing the lower limit on m_u.

Considering only the galaxies for which reliable information can be obtained on the upper mass limit, that is, those with an He I λ2.06 μm/Brγ ratio less than 0.6, we derive an average line ratio of 0.39 with a dispersion of 0.10 (uncertainties on $\alpha^{\rm eff}_{\rm He\,I\,\lambda 2.06}$ not included here) which implies a relatively modest upper mass limit of $30 \pm 3\ M_\odot$. The data obtained on NGC 3256 and NGC 3690–IC 694 also suggest that the upper mass limit is spatially dependent.

It should be stressed that the uncertainty on the effective recombination coefficient, $\alpha^{\rm eff}_{\rm He\,I\,\lambda 2.06}$, has little implications for estimating upper mass limits from He I λ2.06 μm/Brγ ratios. Even if we assume that we have underestimated the value of this coefficient by as much as 50% (we presented an argument in § 3.1 pointing out that possibility), the average upper mass limit of $30 \pm 3\ M_\odot$ inferred above would become $26 \pm 2\ M_\odot$. Such a small difference is hardly surprising given the very steep relationship existing between the He I λ2.06 μm/Brγ ratio and the upper mass limit (cf. Fig. 6). A similar argument applies for the uncertainties related to collisional excitation and dust effects. Irrespective of the magnitude of these two effects, the arguments presented in §§ 3.2 and 3.3 suggest that they would both conspire to make the He I λ2.06 μm/Brγ ratio *higher* for a given effective temperature and therefore also for a given upper mass limit. Thus, it is likely that the upper mass limits given in Table 1 have been systematically *overestimated*. This reinforces the conclusion above that many galaxies have a relatively modest upper mass limit close to $30\ M_\odot$.

It is possible that the line ratio variations observed from one galaxy to another (and within a given galaxy) could be attributed to an age-related phenomenon. Indeed, the He I λ2.06 μm/Brγ ratio calculated from equation (11) is valid only if the starburst is relatively evolved. During the early phase of a starburst event, the He I λ2.06 μm/Brγ ratio is expected to decrease as the most massive stars leave the stellar population first. Thus, in principle, line ratio variations unrelated to the upper mass limit could be expected if the age of the burst varies from one galaxy to another.

We have investigated this evolutionary effect in more detail by using a stellar population synthesis model, based on the evolutionary tracks of Maeder & Meynet (1988). Using this

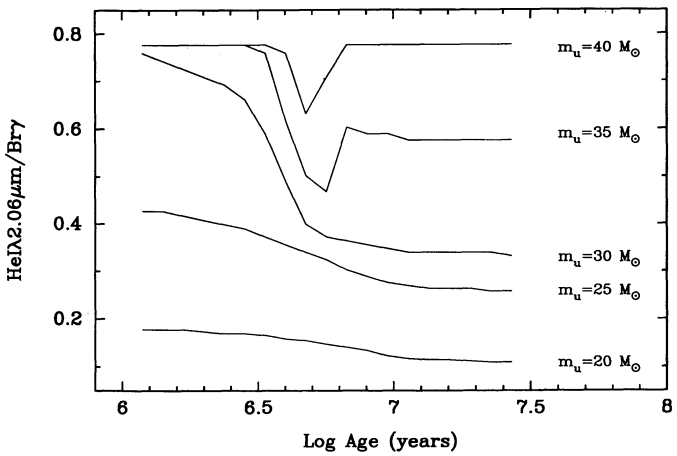

FIG. 7.—Time evolution of the He I λ2.06 μm/Brγ ratio for different upper mass limits, calculated with a stellar synthesis model (*see text*).

model, we calculated the time evolution of the integrated He I λ2.06 μm/Brγ ratio for different upper mass limits, assuming a Salpeter IMF and an exponentially decreasing star formation rate with an arbitrary time scale of 20 million years. The results are displayed in Figure 7. As expected, the line ratio decreases with time but rapidly reaches an equilibrium in less than $\sim$10 million years with asymptotic line ratios similar to those predicted by equation (11).

These calculations show that for a given sample of galaxies experiencing a starburst episode with a supposedly universal upper mass limit, one could expect line ratio variations from one galaxy to another only if there are galaxies in the sample that are younger than $\sim$10 million years, otherwise these variations would necessarily imply that the upper mass limit is not uniquely defined. There are good reasons to believe that the starburst episodes occurring in M82, NGC 1614, NGC 3256A, and NGC 3690A are, at least, older than 10 million years. The evidence is provided by the strong 2.3 μm CO band absorption observed in these galaxies (Doyon 1991; Lester et al. 1990) which suggests the existence of a population of red supergiants. Since these stars appear in the stellar population after $\sim$10 million years, this represents a lower limit for the age of the burst. Thus unless the red supergiants detected in these galaxies are the product of a different starburst episode which created the OB stars responsible for the hydrogen and helium recombination lines, the He I λ2.06 μm/Brγ ratio variations observed from one galaxy to another (see Table 1) probably imply that *the upper mass limit is not a universal parameter of the IMF and probably varies with local physical conditions.*

The relatively low upper mass limit of $\sim 30\ M_\odot$ inferred for half the galaxies in our sample should have important observable consequences. For instance, WR stars should barely exist in these galaxies since the minimum progenitor mass required is 25 $M_\odot$ for a normal or solar metal abundance ($Z = 0.02$) but is as high as 85 $M_\odot$ in low-metallicity ($Z = 0.002$) environments (Maeder 1990). A search for optical WR features (e.g., He II at 4686 Å) would be a good way to determine whether WR stars exist in these galaxies, although high extinction could be a problem in some cases (e.g., NGC 253 and M82). The extinction problem would be minimized by conducting a search in the infrared. The He II emission line at 2.189 μm, a relatively strong feature in many WR stars (especially WN type; e.g. Hillier 1985), would be a very good candidate.

Interestingly, optical WR features have been reported in He 2-10 (Allen, Wright, & Goss 1976; D'Odorico, Rosa, & Wampler 1983; Conti 1991) which is consistent with the upper mass limit greater than 35 $M_\odot$ inferred for this galaxy. However, since this object is likely to have a low metallicity, this would require progenitor masses greater than 40 $M_\odot$ (for $Z \lesssim 0.25\ Z_\odot$) to account for the existence of WR stars. Within the errors, this high upper mass limit is still consistent with the observed He I λ2.06 μm/Brγ ratio. In fact, an upper mass limit as high as 100 $M_\odot$ cannot be excluded for He 2-10 (cf. Fig. 6).

Thus far, WR features have been detected in over three dozen galaxies (Heckman, Armus, & Miley 1987; Armus, Heckman, & Miley 1988; Conti 1991), including He 2-10. It would be interesting to obtain near-infrared spectra of the other objects. From the existence of a WR population, we can predict that the average He I λ2.06 μm/Brγ ratio should be relatively high (>0.5) if stars more massive than 30 $M_\odot$ exist in these galaxies. Such measurements would, at least, constrain the range of possible progenitor masses for WR stars.

Although we have presented evidence that the He I λ2.06 μm/Brγ ratio can be used as a reliable probe of the massive stellar population, this technique has serious limitations for predicting the upper mass limit when the ratio becomes higher than $\sim$0.6 ($m_u \gtrsim 40$), due to uncertainties in both the theoretical ratio and the helium abundance, and also because the ratio saturates. Uncertainties in the theoretical ratio should be removed in the near future when reliable calculations of the He I λ2.06 μm recombination coefficient become available.

5. SUMMARY AND CONCLUSIONS

We have analyzed near-infrared spectra of star-forming galaxies which show strong Brγ and He I λ2.06 μm emission. These lines are interpreted as arising from ionization by recently formed OB stars, and a theoretical relationship between the He I λ2.06 μm/Brγ ratio and effective temperature is derived. The ratio is a steep function of the temperature, a feature that can be used to determine, independently of the distance, the spectral type of the exciting star in H II regions.

We have shown that the steep dependence between the He I λ2.06 μm/Brγ ratio and temperature can be translated into a strong constraint on the upper mass limit of the IMF in starbursts, but reliable only for upper mass limits less than $\sim 40\ M_\odot$. In general, the upper mass limit inferred from the He I λ2.06 μm/Brγ ratio varies from one galaxy to another and appears to show spatial variation as well. Age-related phenomena can be ruled out as the most likely explanation for these variations. They suggest instead that the upper mass limit is not a universal parameter of the IMF and probably varies with local physical conditions. Half the galaxies studied in this paper have relatively low upper mass limits, near 30 $M_\odot$.

It is a pleasure to thank Dolores Walther, Joel Aycock, and Thor Wold for their invaluable skill and efficiency in operating the telescope. We also thank the referee Kurt Anderson, for a detailed discussion on the excitation of helium within ionized regions and for constructive criticism which improved the presentation of this paper. R. D. was financially supported by postgraduate fellowships from the Natural Science and Engineering Research Council of Canada and the Canadian chapter of IODE. P. J. P. is grateful to SERC fellowships for financial support during the period when much of this work was carried out.

REFERENCES

Allen, D. A., Wright, A. E., & Goss, W. M. 1976, MNRAS, 177, 91
Armus, L., Heckman, T. M., & Miley, G. K. 1988, ApJ, 326, L45
Brocklehurst, M. 1972, MNRAS, 157, 211
Chini, R., Krügel, E., & Wargau, W. 1987, A&A, 181, 378
Churchwell, E., Wolfire, M. G., & Wood, D. O. S. 1990, ApJ, 354, 247
Conti, P. S. 1991, ApJ, 377, 115
D'Odorico, S., Rosa, M., & Wampler, E. J. 1983, A&AS, 53, 97
Doyon, R. 1991, Ph.D. thesis, Imperial College, Univ. London
Doyon, R., Joseph, R. D., & Wright, G. S. 1992, in preparation
Draine, B. T. 1985, ApJS, 57, 587
Draine, B. T., & Lee, H. M. 1984, ApJ, 285, 89
Gehrz, R. D., Sramek, R. A., & Weedman, D. N. 1983, ApJ, 267, 551
Heckman, T. M., Armus, L., & Miley, G. K. 1987, AJ, 93, 276
Hillier, D. J. 1985, AJ, 90, 1514
Hummer, D. G., & Storey, P. J. 1987, MNRAS, 224, 801
Kennicutt, R. L., Keel, V. C., van der Hulst, J. M., Hummel, E., & Roettiger, K. A. 1987, A&A, 93, 1011
Kurucz, R. L. 1979, ApJS, 40, 1
Landolt-Börnstein. 1982, Astronomy & Astrophysics, 2B, Star & Star Clusters, ed. K. Schiaffers & H. H. Voigt (Berlin: Springer)
Lester, D. F., Carr, J. S., Joy, M., & Gaffney, N. 1990, ApJ, 352, 544
Maeder, A. 1990, A&AS, 84, 139
Maeder, A., & Meynet, G. 1988, A&AS, 76, 411
Mateo, M. 1988, ApJ, 331, 261
Mathis, J. S. 1986, PASP, 98, 995
Mathis, J. S., Rumpl, W., & Nordsieck, K. H. 1977, ApJ, 244, 483
Miller, G. E., & Scalo, J. M. 1979, ApJS, 41, 513
Olofsson, K. 1989, A&AS, 80, 317
Osterbrock, D. E. 1989, Astrophysics of Gaseous Nebulae and Active Galactic Nuclei (Mill Valley, CA: University Science Books)
Panagia, N. 1974, ApJ, 192, 221
Peimbert, M., & Torres-Peimbert, S. 1971, Bol. Obs. Ton. y Tac., 6, 21
Puxley, P. J. 1988, Ph.D. thesis, Univ. Edinburgh
Puxley, P. J., Brand, P. W. J. L., Moore, T. J. T., Mountain, C. M. Nakai, N., & Yamashita, T. 1989, ApJ, 345, 163
Puxley, P. J., Hawarden, T. G., & Mountain, C. M. 1990, ApJ, 364, 77
Rieke, G. H., Lebofsky, M. J., Thompson, R. I., Low, F. J., & Tokunaga, A. T. 1980, ApJ, 238, 24
Rieke, G. H., Lebofsky, M. J., & Walker, C. E. 1988, ApJ, 325, 679
Rubin, R. H. 1985, ApJS, 57, 349
Salpeter, E. E. 1955, ApJ, 121, 161
———. 1977, ARA&A, 15, 267
Scalo, J. M. 1986, Fund. Cosmic Phys., 11, 1
———. 1987, in Starbursts and Galaxy Evolution, ed. T. X. Thuan, T. Montmerle, & J. Tran Tranh Van (Paris: Éditions Frontières), 445
———. 1989, in Windows on Galaxies, ed. A. Renzini, G. Fabianno, & J. S. Gallagher (Dordrecht: Kluwer), 125
Sekiguchi, K., & Anderson, K. S. 1987, AJ, 94, 644
Thompson, R. I., & Tokunaga, A. T. 1980, ApJ, 235, 889
Tielens, A. G. G. M., & de Jong, T. 1979, A&A, 75, 326
Treffers, R. R., Fink, U., Larson, H. P., & Gauthier, III, T. N. 1976, ApJ, 209, 793
Wood, D. O. S., & Churchwell, E. 1989, ApJS, 69, 831
Wright, G. S., Joseph, R. D., Robertson, N. A., James, P. A., & Meikle, W. P. S. 1988, MNRAS, 233, 1
Wynn-Williams, C. G., Becklin, E. E., Matthews, K., & Neugebauer, G. 1978, MNRAS, 183, 237
Zinnecker, H. 1987, in Proc. 10th European Regional Astronomy Meeting of the IAU, Vol. 4, Evolution of Galaxies, ed. L. Palous, (Prague: Publ. Astron. Inst. Czech. Acad. Sci.), 77